



Symmetry relationship of quantum tunneling and its applicationsP. W. Wen ¹, C. J. Lin ^{1,2,*}, H. M. Jia,¹ L. Yang,¹ N. R. Ma,¹ and F. Yang¹¹*China Institute of Atomic Energy, Beijing 102413, China*²*College of Physics and Technology, Guangxi Normal University, Guilin 541004, China*

(Received 9 March 2024; accepted 2 May 2024; published 3 June 2024)

Quantum mechanics serves as the fundamental cornerstone for numerous areas of research. Finding simple and analytical quantum transmission coefficients for potentials is a rare occurrence. Notably, we have discovered a readily provable yet unreported symmetry tunneling law. For an infinite parabolic potential, it can be proved analytically that the sum of the one-dimensional tunneling probabilities at incident energies equal to the barrier height plus or minus any energy deviation is consistently 1. Based on this relationship, the original WKB approximation and the Kemble's formula can be generalized to the above-barrier energy region in a simplified but more accurate manner, referred to as the symmetric WKB approach in this context. For the realistic potential between two nuclei, numerical results demonstrate that the symmetry relationship at the above-barrier energy region and the sub-barrier energy is also well satisfied, as well as in the cases of the multichannel WKB method. The symmetry tunneling law has been effectively extended to the Eckart potential as well. Such symmetry in tunneling may have universal characteristics but its underlying reason remains to be uncovered, which may help us to further understand the quantum mechanisms.

DOI: [10.1103/PhysRevC.109.064602](https://doi.org/10.1103/PhysRevC.109.064602)**I. INTRODUCTION**

In quantum mechanics, a particle with matter wave structure can penetrate through a potential barrier with the barrier height higher than its kinetic energy. This microscopic quantum tunneling phenomenon has significant applications on atomic, molecular, and nuclear physics [1,2]. With the development of the engineering and manufacturing, the current possible controlling quantum tunnelings have been a central issue in many emerging new fields of the nanoscopic and mesoscopic scales, such as the Josephson junctions [3,4]. In nuclear reactions, quantum tunneling happens in the cluster decay, fission, and fusion reactions and so on [5–11]. How to determine the quantum penetration probability is a critical problem among these phenomena.

Given the rarity of analytical solutions for quantum tunneling in many potential systems, one primary approach involves solving the Schrödinger equations under specific boundary conditions via numerical simulations [12,13]. The realistic potential between two nuclei consists of contributions from Coulomb interaction, nuclear interaction, and centrifugal interaction. The barrier formed by this potential plays a vital role in nuclear reactions, which has been systematically studied in many studies [14–16]. The penetration probability through this barrier can be obtained by solving the adiabatic Schrödinger equation using a complex potential (the optical potential) [17] or adopting the incoming wave boundary condition [18]. For the latter case, a strong absorption condition inside the Coulomb barrier is imposed in the incoming wave

boundary condition. The plane wave without reflection at the pocket minimum is adopted, and the asymptotic Coulomb function is used to determine the boundary condition at the long tail of the potential. For multichannel potential penetration, the adiabatic coupled-channel equation is solved to obtain the quantum tunneling probability. This method has been used in many previous studies [15,19–22].

The computation time will increase dramatically when more reaction channels are considered in the coupled-channel calculations [23]. The semiclassical approaches based on the WKB method or the path integral approach will give accurate estimations [24]. For complex systems such as dissipative tunneling, the semiclassical method is the main feasible tool due to the difficulty and time-consuming nature of numerically exact solutions [3,25], which will also provide a better understanding of physical intuition.

There is a long-standing problem for the application of the WKB approximation on the above-barrier energy tunneling. The standard method of applying the WKB penetration formula to the above-barrier energy is to extend the integral range to the complex plane [12,26,27]. However, this method is not straightforward. The most popular used formula in nuclear decay, fission, and fusion reactions is still the original WKB formula [see Eq. (1) below] or Kemble's improved version [28–32].

In this work, a symmetry relationship in tunneling through the potential barrier of two nuclei is demonstrated, which can be applied to solve the above-barrier tunneling problem simply. The present paper is organized as follows. In Sec. II, the theoretical framework is briefly described. Section III presents the numerical calculations on two light fusion reaction systems. Finally, the summary of the article is given in Sec. IV.

*cjlin@ciae.ac.cn

II. THEORETICAL FRAMEWORK

A. Single-channel WKB formula

The WKB transmission probability through the barrier of the l partial-wave at incident energy E is written as

$$P_l^{\text{WKB}}(E) = \exp[-2\Phi_l^{\text{WKB}}(E)], \quad (1)$$

where

$$\Phi_l^{\text{WKB}}(E) = \int_{r_1}^{r_2} k_l(r) dr. \quad (2)$$

The r_1 and r_2 in the above integral are the classical turning points where the potential energy $V_l(r)$ equals to E . The wave number in the above formula is expressed as $k_l(r) = \sqrt{2\mu[V_l(r) - E]/\hbar^2}$, where $\mu = m_1 m_2 / (m_1 + m_2)$ is the reduced mass of the projectile and the target with masses m_1 and m_2 , respectively. Taking the parabolic potential as an example, when E of the interaction system is equal to the barrier height V_B , r_1 tends to be equal to r_2 in Eq. (2), so that $\Phi_l^{\text{WKB}}(E) = 0$ and $P_l^{\text{WKB}}(E) = 1$. However, the analytical results will give $P = 0.5$ [12]. An improvement to the WKB formula was given by Kemble [33], i.e.,

$$P_l(E) = 1 / \{1 + \exp[2\Phi_l^{\text{WKB}}(E)]\}. \quad (3)$$

Based on this formula, the tunneling probability at the above-barrier energy will always be 0.5. Therefore, it cannot be used for above-barrier energies, where the tunneling probability tends to be 1.0.

The parabolic potential plays an essential role in quantum mechanics [12] and supersymmetric quantum mechanics [34]. Many calculations could be significantly simplified by adopting this potential, which enriches our understanding of the microscopic quantum world. The nuclear potential is often treated as an approximation of the inverse parabolic potential, which can be expressed as

$$V(x) = V_B - \frac{1}{2}\mu\omega^2 x^2, \quad (4)$$

where $\hbar\omega$ is the curvature of the potential. The tunneling probability of this potential can be analytically solved [12,35], namely,

$$P(E) = \frac{1}{1 + \exp\left[\frac{2\pi}{\hbar\omega}(V_B - E)\right]}, \quad (5)$$

which is often called the Hill-Wheeler (HW) formula. Due to its simplicity, this HW penetration formula is widely used [14,36–38]. For the parabolic potential, a special relationship between the sub-barrier tunneling probability and the above-barrier tunneling probability can be proved, namely,

$$\begin{aligned} & P(V_B + \delta E) + P(V_B - \delta E) \\ &= \frac{1}{1 + \exp\left[\frac{2\pi}{\hbar\omega}(V_B - V_B - \delta E)\right]} \\ &+ \frac{1}{1 + \exp\left[\frac{2\pi}{\hbar\omega}(V_B - V_B + \delta E)\right]} \\ &= 1. \end{aligned} \quad (6)$$

It is natural to derive that, when $\delta E = 0$, $P(V_B) = 0.5$. The above feature of the penetration through the parabolic

potential is irrelevant to the width or curvature of the potential, unlike that of the square potential barrier or the Eckart potential [12]. However, it should be noted this is not usually the case for any symmetric parabolic potential barrier. Equation (6) is only fulfilled by solving the Schrödinger equation under infinite inverted parabolic potential boundary conditions. For a finite parabolic potential, if the plane-wave boundary conditions are adopted, the relationship Eq. (6) will be subject to small disturbances. Because the shape of the nuclear potential is not exactly parabolic, and the boundary condition is also not the same as the above case, the penetration probability at incident energy equal to the barrier height is also disturbed, as well as the symmetry relationship Eq. (6).

At the above-barrier energy, the penetration probability is close to 1. The cross sections concerned are not as sensitive to the penetration probability as that of sub-barrier energy. Considering also the existence of the symmetric relationship between sub-barrier and above-barrier transmission probabilities shown in Eq. (6), a new simple formula is proposed for applying the WKB formula to the above-barrier energy region in this work. The probability above the barrier energy can be deduced reversely according to Eq. (6) from Kemble's formula, Eq. (3), namely,

$$\begin{aligned} P_l(E) &= 1 - \frac{1}{1 + \exp[2\Phi_l^{\text{WKB}}(2V_B(\ell) - E)]} \\ &= \frac{1}{1 + \exp[-2\Phi_l^{\text{WKB}}(2V_B(\ell) - E)]}, \\ &= 1 - P_l(2V_B(\ell) - E), \end{aligned} \quad (7)$$

when $E > V_B(\ell)$, with $V_B(\ell)$ being the barrier height at the ℓ th angular momentum. The turning point used in the above formula is obtained as the same one as when the incident energy is $2V_B(\ell) - E$. This formula is named the symmetric WKB (SymWKB) method. By solving the below-barrier tunneling probability using the WKB formula, according to the above equation, the above-barrier tunneling probability can be derived directly without further calculations. For instance, if the barrier V_B is 10 MeV, the tunneling probability by WKB at $E = 8$ MeV is 0.4, then the tunneling probability at the symmetry position relative to the barrier, i.e., $E = 12$ MeV, would be $1 - 0.4 = 0.6$.

Finally, the total capture cross section is expressed as a sum over partial waves at the center-of-mass energy E , which is

$$\sigma_f(E) = \sum_l \sigma_l(E) = \frac{\pi}{k_0^2} \sum_l (2l + 1) P_l(E), \quad (8)$$

where the incident wave number is expressed as $k_0 = \sqrt{2\mu E/\hbar^2}$.

B. Multichannel WKB formula

The multichannel WKB formula can be derived based on the local transmission matrix method [24,39]. It is obtained

from the coupled-channels equations as follows:

$$-\frac{\hbar^2}{2v} \frac{d^2}{dx^2} u_{nm_0}(x) + \sum_m [V_{nm}(x) + \epsilon_m \delta_{n,m} - E] u_{nm_0}(x) = 0, \quad (9)$$

where ϵ_n is the excitation energy for the n th channel. $u_{nm_0}(x)$ is the wave-function matrix, where n refers to the channel and n_0 specifies the incident channel. The incoming wave boundary conditions for $u_{nm_0}(x)$ are given by

$$u_{nm_0}(x) \rightarrow T_{nm_0} e^{-ik_n x} \quad (x \rightarrow -\infty), \quad (10)$$

$$\rightarrow \delta_{nm_0} e^{-ik_n x} + R_{nm_0} e^{ik_n x} \quad (x \rightarrow \infty), \quad (11)$$

where $k_n = \sqrt{2m(E - \epsilon_n)/\hbar^2}$ is the wave number for the n th channel.

After some approximations, see more details in Ref. [24], the multichannel WKB tunneling probability is obtained as

$$P = \sum_n \left| \langle n | \prod_i \left[\sum_m |m(x_i)\rangle e^{iq_m(x_i)\Delta x} \langle m(x_i)| \right] | n_0 \rangle \right|^2, \quad (12)$$

where $\mathbf{q}(x) = \{2\mu[E - \mathbf{W}(x)]/\hbar^2\}^{1/2}$, with $W_{nm}(x) = V_{nm}(x) + \epsilon_n \delta_{n,m}$. $|m(x)\rangle$ is the eigenvector of the matrix $\mathbf{W}(x)$ with the eigenvalue of $\lambda_m(x)$, and $q_m(x) \equiv \sqrt{2m[E - \lambda_m(x)]/\hbar^2}$.

For a one-channel problem, Eq. (12) is equal to the original WKB formula in Eq. (2). For a multichannel problem, the drawback of the WKB equation is also inherited. The tunneling probability calculated by Eq. (12) is generally higher than the exact value when the incident energy is near the eigenbarriers. Two prescriptions are proposed to deal with this problem, including the dynamical norm method and the eigenchannel approach [24]. Since the second approach was proved to agree with experimental data better than the first one, we try to test it in the following.

In the eigenchannel approach, the penetrability is obtained by a weighted sum of the penetrability for each eigenbarrier,

$$P(E) = \sum_{n=0}^{N-1} w_n P_n(E), \quad (13)$$

where $P_n(E)$ is the penetrability for the eigenpotential $\lambda_n(x)$. In the weight factors, w_n are assumed independent of the distance and usually predicted at the barrier positions [40–42].

In Ref. [24], the coordinate dependence of $\mathbf{W}(x)$ is properly taken into account assuming that it is independent of energy. The procedure is as follows. Starting from the lowest eigenbarrier B_0 and considering the original one channel WKB approximation $P_0(B_0) = 1$, it can be obtained from Eq. (13) that $P(B_0) \sim w_0 P_0(B_0) \sim w_0$, when $E = B_0$. Then the first weight factor w_0 for the lowest eigenbarrier is obtained. Repeat this procedure $N - 1$ times; the weight factor for the $(k + 1)$ th eigenbarrier will be

$$w_k = P_{\text{WKB}}(B_k) - \sum_{i=0}^{k-1} w_i, \quad (14)$$

where B_k is the barrier height of the $(k + 1)$ th eigenbarrier, and P_{WKB} is the multichannel tunneling probability calculated

by Eq. (12). The weight factor for the highest eigenbarrier $\lambda_{N-1}(x)$ is evaluated as

$$w_{N-1} = 1 - \sum_{i=0}^{N-2} w_i, \quad (15)$$

in order to keep the unitarity.

After the penetrability is written as Eq. (13), the multi-channel problem can be reduced to a summation of a different one-channel problem. We can substitute the $P_n(E)$ with the exact one, which can be obtained from solving the one-channel Schrödinger equations. In this work, we test if $P_n(E)$ can be substituted with the SymWKB formula, Eq. (7).

III. RESULTS AND DISCUSSIONS

A. Test of single-channel WKB formula with AW-type WS potential

The fusion of the symmetric $^{28}\text{Si} + ^{28}\text{Si}$ reaction and the asymmetric $^{17}\text{O} + ^{144}\text{Sm}$ reaction are used as examples to test Eq. (7). At first, we test the tunneling probability with the Akyüz-Winther (AW)-type Woods-Saxon (WS) potential [45], which is widely used in different reactions [46]. It gives the potential parameters V_0 , R_0 , and a_0 as 53.759 MeV, 7.108 fm, and 0.6345 fm for $^{28}\text{Si} + ^{28}\text{Si}$ and 62.130 MeV, 9.195 fm, and 0.654 fm for $^{17}\text{O} + ^{144}\text{Sm}$. The angular momentum is taken from zero to the value where the tunneling probability is too weak to make contributions.

In Figs. 1(a) and 1(b), the penetration probability at zero angular momentum is plotted at linear coordinates and logarithmic coordinates, and the fusion cross sections for $^{28}\text{Si} + ^{28}\text{Si}$ are presented in Figs. 1(c) and 1(d) at different coordinates, respectively. In Fig. 1, labels SC and WKB denote the single-channel calculation by the quantum tunneling method [47] and the WKB formula, Eq. (1). The results labeled as SymWKB represent that above-barrier penetration probabilities and cross sections are deduced from the sub-barrier predictions according to Eq. (6). The results of the HW formula in Eq. (5) are shown as dashed lines.

From Fig. 1(a), it can be seen that the results of Exact, HW, SymWKB are almost overlapped, which demonstrates that Eq. (6) applies well to this potential. The calculated penetration probability of the original WKB formula quickly increases up to 1 near the barrier energy and deviates a lot from other calculations, and the semiclassical SymWKB results are still almost undistinguished from the results of Exact. This proves the applicability of Eq. (7). Meanwhile, according to the results shown in Fig. 1(b), the HW results are significantly higher than all other results. This is due to the parabolic approximation used in the HW formula, which decreases the barrier width and tends to overestimate the tunneling probability.

After summing up the partial fusion cross sections at each angular momentum, the total cross sections can be obtained. Comparing the cross sections shown in Figs. 1(c) and 1(d), it can be seen that the results calculated by the WKB method overestimate the total fusion cross sections at the

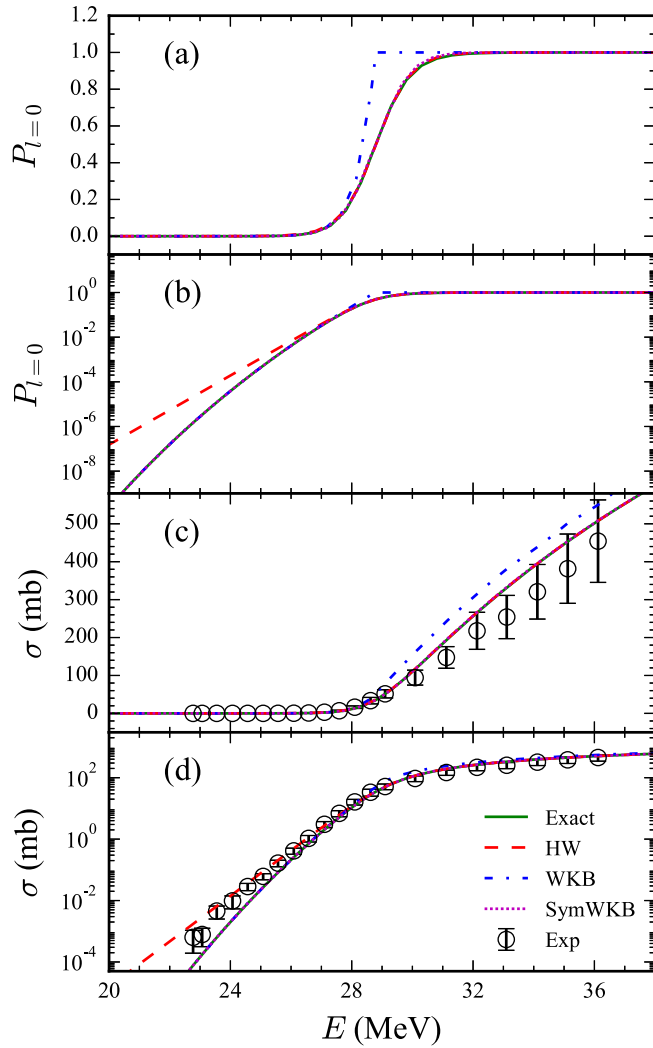


FIG. 1. The single-channel penetration probability $P_{l=0}$ with zero angular momentum at linear coordinates (a) and logarithmic coordinates (b), and fusion cross sections at linear coordinates (c) and logarithmic coordinates (d) for the $^{28}\text{Si} + ^{28}\text{Si}$ reaction under the AW-type Woods-Saxon potential. The experimental fusion cross sections (open circles) are from Ref. [43]. The results by numerically solving the quantum equation (Exact) are shown as the solid lines. The WKB prediction and its reversed calculation SymWKB are presented as densely dashed and densely dotted lines. The results of the Hill-Wheeler formula are shown as dashed lines.

above-barrier energy. The situation of the calculated cross sections by different methods is similar to that of tunneling probability. At the above-barrier energy region, the results of the Exact, HW and SymWKB methods are overlapped and are smaller than those of the WKB method. In the sub-barrier energy region, the WKB method makes excellent predictions that coincide with those of the Exact method, as well as those of the SymWKB method. The results of HW overestimate a lot compared to the Exact results. The above results demonstrate the accuracy of semiclassical SymWKB results, which is quite close to the accuracy of the exact quantum mechanical results in this case.

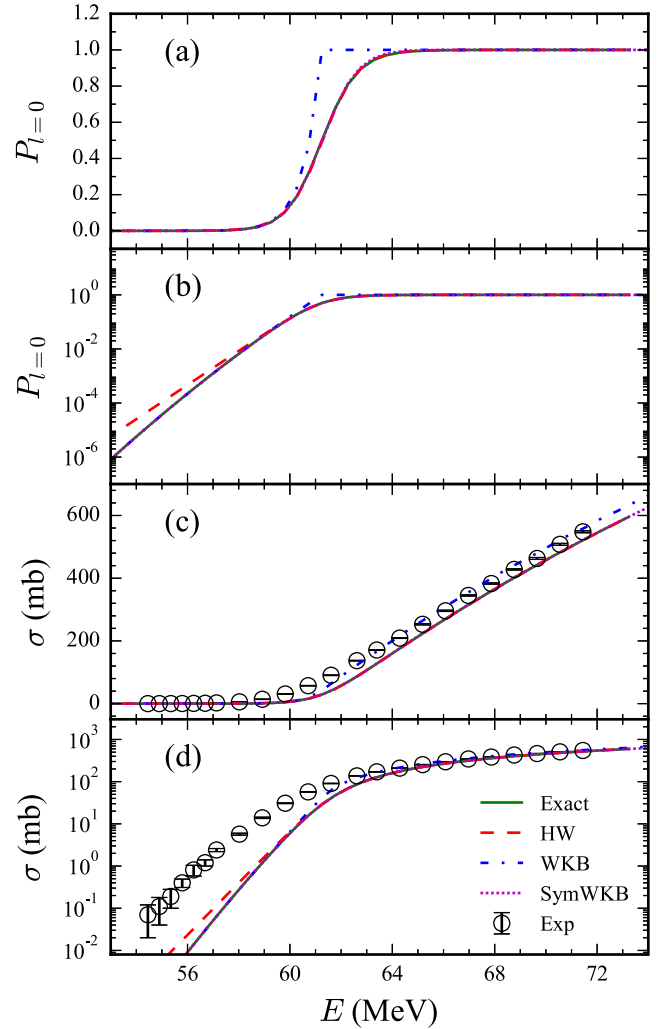


FIG. 2. Same as Fig. 1 but for the $^{17}\text{O} + ^{144}\text{Sm}$ fusion reaction under the AW-type Woods-Saxon potential. The experimental fusion cross sections (open circles) are from Ref. [44].

The penetration probability at zero angular momentum and the fusion cross sections for the $^{17}\text{O} + ^{144}\text{Sm}$ fusion reaction are given in Figs. 2(a) and 2(b) and Figs. 2(c) and 2(d), respectively. This is a very asymmetric reaction compared to the previous one. Similar to the results shown in Fig. 1, the tunneling probabilities and the cross sections predicted by the original WKB method are larger than those of other methods at the above-barrier energy region. Moreover, the results calculated by the Exact, HW and SymWKB methods are also overlapped. At the sub-barrier energy region, the HW formula tends to overestimate the sub-barrier fusion cross sections. Similarly, the Wong formula which is derived from the HW formula has also been shown to overstate the results [19,26]. The WKB predictions at the sub-barrier energy region are undistinguished from the exact quantum calculation based on the calculations in this work. This character makes the SymWKB method a more suitable simple tool for the one-channel tunneling problem at both the above-barrier and the sub-barrier energy regions.

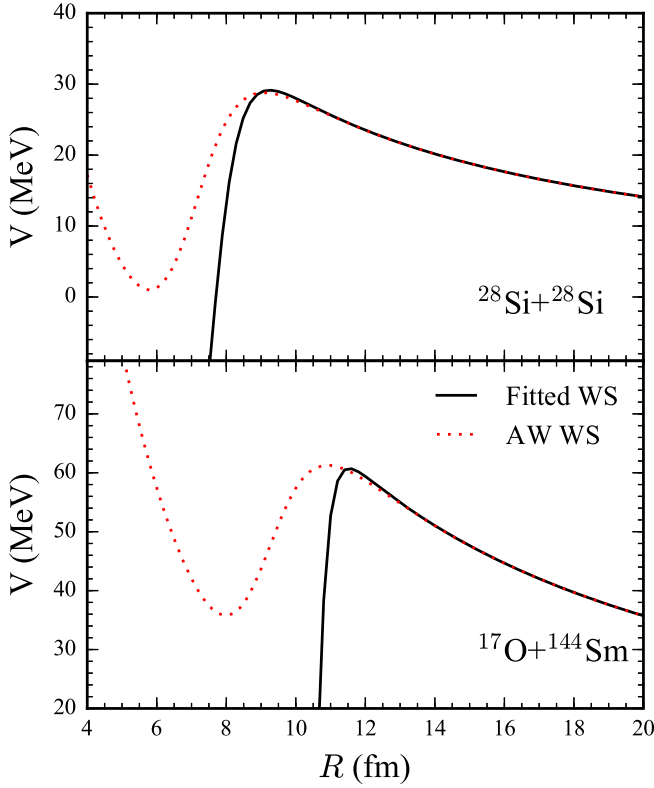


FIG. 3. The ion-ion potential V for reactions $^{28}\text{Si} + ^{28}\text{Si}$ and $^{17}\text{O} + ^{144}\text{Sm}$ at zero angular momentum. A dotted line represents the results of the AW-type Woods-Saxon nuclear potential plus a dot Coulomb potential, and the nuclear potential containing a fitted Woods-Saxon potential is shown as a solid line.

B. Test of single-channel WKB formula with general WS potential

To test Eq. (7) for general cases, we test the fitted Woods-Saxon potential in this step. We obtain the parameters of the Woods-Saxon potential by fitting the experimental data directly, using the exact quantum model without coupling (Exact) [20,47]. Due to the strong couplings in these two nuclear reaction systems [43,44], unusual potential parameters are obtained by considering only one channel. The fitted Woods-Saxon nuclear potential parameters V_0 , R_0 , and a_0 are 98.522 MeV, 7.483 fm, and 0.415 fm for the reaction $^{28}\text{Si} + ^{28}\text{Si}$ and 267.930 MeV, 10.315 fm, and 0.226 fm for the reaction $^{17}\text{O} + ^{144}\text{Sm}$. The comparisons of the fitted potential and the standard AW-type potential for these two reactions are plotted in Fig. 3. It can be seen that the fitted potential parameters deviate a lot compared to the standard AW-type potential. The solid lines in the figure clearly show that the shape of the fitted Woods-Saxon potential is far from a parabolic one, especially for the reaction $^{17}\text{O} + ^{144}\text{Sm}$. The fitted potential of this reaction decreases sharply inside the potential pocket. In Figs. 4 and 5, the penetration probability at zero angular momentum and the fusion cross sections at linear coordinates and logarithmic coordinates are presented for $^{28}\text{Si} + ^{28}\text{Si}$ and $^{17}\text{O} + ^{144}\text{Sm}$, respectively.

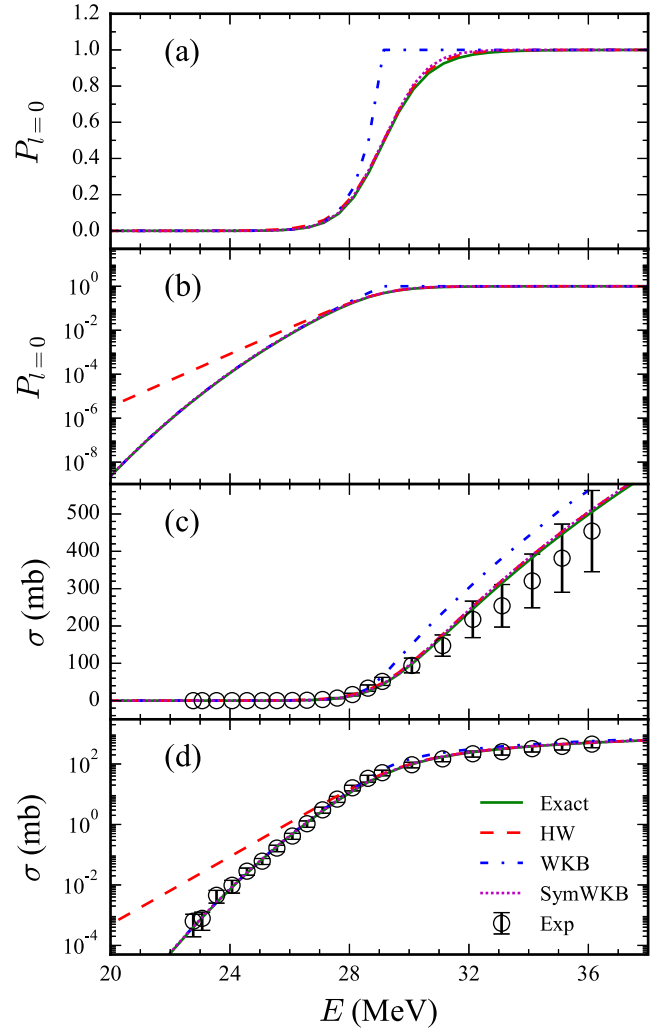


FIG. 4. Same as Fig. 1 but for the $^{28}\text{Si} + ^{28}\text{Si}$ reaction under the fitted Woods-Saxon potential.

From Fig. 4, it can be seen that results of the Exact and SymWKB methods are almost overlapped at all subplots, which demonstrates that Eqs. (6) and (7) apply well to this potential. The calculated penetration probability of the original WKB formula quickly increases up to 1 near the barrier energy and deviates a lot from other calculations. The results that are shown in Figs. 4(a) and 4(c) demonstrate that calculations by the WKB method still highly overestimate the total fusion cross sections. In the sub-barrier energy region, WKB and SymWKB make excellent predictions that coincide with the Exact method. With this fitted potential, the deviation of the WKB and the Exact results are significantly larger than that shown in Fig. 1, as well as the deviation of the HW and the Exact results. This is because the new potential deviates from parabolic further in the fitting process.

The results of the reaction $^{17}\text{O} + ^{144}\text{Sm}$ are given in Fig. 5. In this figure, the results calculated by the SymWKB method are very close to those of the Exact method at the above-barrier energy region. Similar to that of the previous reaction, the cross sections are overlapped at the sub-barrier energy

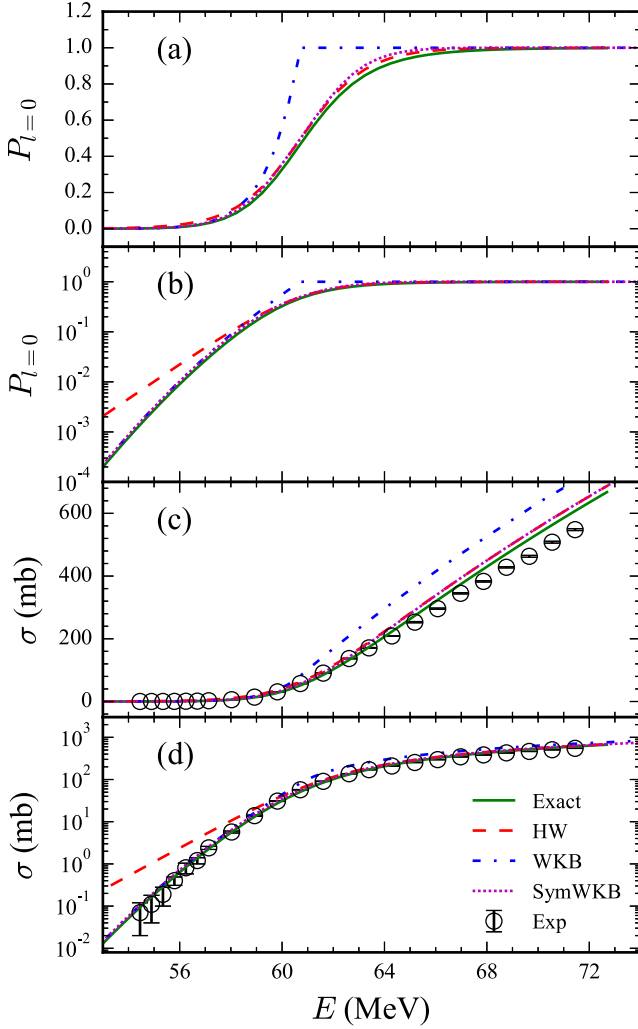


FIG. 5. Same as Fig. 1 but for the $^{17}\text{O} + ^{144}\text{Sm}$ fusion reaction under the fitted Woods-Saxon potential.

region. Moreover, the results by the WKB and HW formulas deviate more obviously from the Exact results than those shown in Fig. 2. The SymWKB results are still good approximations compared to the Exact method. Similar to the HW formula and other simple formulas, it should be noted that Eqs. (6) and (7) cannot be used for the prediction of very heavy and very light fusion reactions, where other mechanisms such as the deep-inelastic scattering, incomplete fusion, or the oscillations and resonance structures appear [6,28,48].

C. Test of multichannel WKB formula

In this work, we adopt the same coupled potential as that tested in Ref. [24] for the convenience of comparison. Considering a three-level problem, the coupling potential is expressed as

$$\mathbf{W}(x) = \begin{pmatrix} V(x) & F(x) & 0 \\ F(x) & V(x) + \epsilon & F(x) \\ 0 & F(x) & V(x) + 2\epsilon \end{pmatrix}, \quad (16)$$

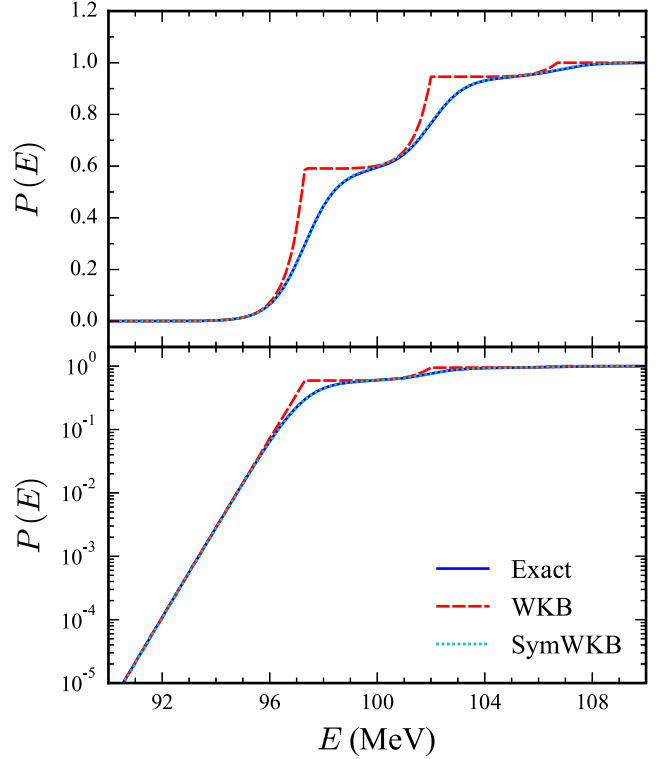


FIG. 6. Multichannel calculation of cross sections at linear coordinates (a) and logarithmic coordinates (b) for a three-level coupled potential in Eq. (16). The solid lines denote the Exact results by solving the coupled-channels equation. The multichannel calculation with the WKB formula Eq. (12) is denoted as the densely dashed lines. The multichannel prediction with the eigenchannel approximation [Eq. (13)] and the SymWKB formula [Eq. (7)] are presented as the dotted lines.

with

$$V(x) = V_0 e^{-x^2/2s^2}, \quad (17)$$

$$F(x) = F_0 e^{-x^2/2s_f^2}, \quad (18)$$

where $V_0 = 100$ MeV, $F_0 = 3$ MeV, and $s = s_f = 3$ fm, which are chosen to simulate the potential between two ^{58}Ni nuclei. The excitation energy ϵ and the reduced mass μ are set as 2 MeV and $29m_N$, respectively, where $m_N = 938$ MeV is the nucleon mass. The barrier height for the uncoupled barrier is V_0 . The three eigenbarriers $\lambda_i(x)$ are 97.31, 102.0, and 106.7 MeV, respectively, which are obtained by diagonalizing $\mathbf{W}(x)$ at the barrier position. In the following calculations, we substitute the $P_i(E)$ in Eq. (13) with the SymWKB formula [Eq. (7)] to test the multichannel WKB formula.

The results are shown in Fig. 6. Similar to the single-channel case, the original WKB formula highly overestimates the tunneling probability at the near-eigenbarrier energy regions, and results predicted by the SymWKB formula for multichannel calculations agree with the Exact results very well. The Exact results used in this work are obtained by our recently developed program KANTBP 3.1 (CCFULL-FEM)

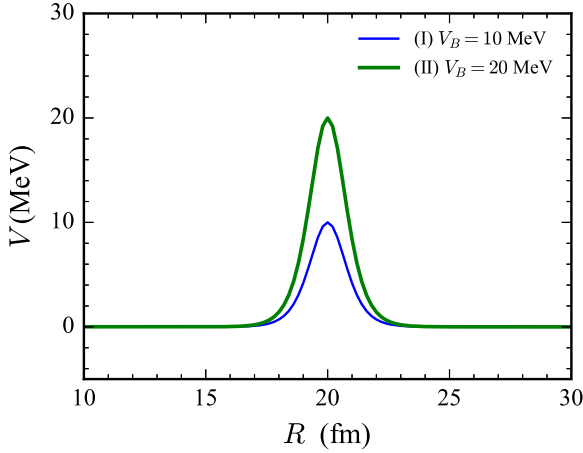


FIG. 7. The Eckart potential V in Eq. (19). The thin and thick solid lines represent two cases where (I) $V_B = 10$ MeV and (II) $V_B = 20$ MeV.

[20,21,49–51], which solves the coupled-channels equation with a very high-accuracy finite-element method. The calculations indicate that the SymWKB formula is suitable for multichannel tunneling calculations. This method takes much less computational power than solving the coupled-channels equation, which will be more suitable for the very large dimensional multichannel tunneling calculations.

D. Extension of the symmetry law to the Eckart potential

Another well-known one-dimensional potential that has an analytic solution of penetrability is the Eckart potential. This potential has been applied to various nuclear physical research [52,53]. Its analytical tunneling probability has been listed in various quantum mechanic textbooks such as Ref. [12]. It would be interesting to check the symmetric law of the above-barrier and the sub-barrier tunneling probabilities. In this subsection, we take the potential form as

$$V(R) = V_B / \cosh^2(R - R_B), \quad (19)$$

where V_B and R_B are the potential barrier height and radius. If $8mV_B/\hbar^2 > 1$, the analytic solution is

$$P(E) = \frac{\sinh^2(\pi k)}{\sinh^2(\pi k) + \cosh^2\left[\frac{1}{2}\pi\sqrt{8mV_B/\hbar^2 - 1}\right]}, \quad (20)$$

where $k = \sqrt{2mE/\hbar^2}$. To be simple, $2m/\hbar^2$ is set as $1 \text{ MeV}^{-1} \text{ fm}^{-2}$, and R_B is set as 20 fm here. Two cases are tested in this work including (I) $V_B = 10$ MeV and (II) $V_B = 20$ MeV. The shapes of the potential are plotted in Fig. 7. The tunneling probability by the analytic solution in Eq. (20) is shown as the solid lines. One can see that, when $E = V_B$, the tunneling probabilities are 0.563 and 0.544 for cases (I) and (II). Therefore, the symmetry law $P(V_B + \delta E) + P(V_B - \delta E) = 1$ is obviously not fulfilled. However, one could slightly adjust the law as

$$P(V_B + \delta E) + aP(V_B - \delta E) = 1. \quad (21)$$

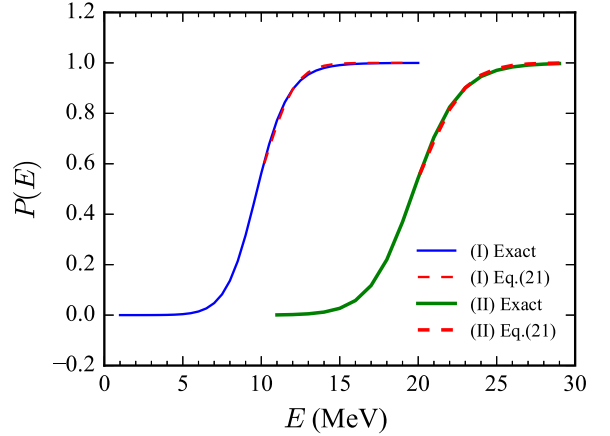


FIG. 8. The tunneling probability for the Eckart potential. The Exact results are shown by the thin and thick solid lines, while the results by the law in Eq. (21) are shown as the thin and thick dashed lines for the two cases where (I) $V_B = 10$ MeV and (II) $V_B = 20$ MeV.

It amounts to scaling the new tunneling probability close to 0.5 at the barrier position, and the critical step is to determine the coefficient a . Submitting the tunneling probability at $\delta E = 0$, namely, $E = V_B$, one could get the value of a as 0.776 and 0.838 based on the above equation. The results by Eq. (21) are shown in Fig. 8. It is remarkable to find that the above-barrier tunneling probabilities transformed by the sub-barrier value agree well, although not exactly, with the analytic solutions. This may be due to the close shape of this potential to the inverse parabolic potential, and it would be interesting to check more potentials later about the application range and find the deep reason for the symmetry laws.

IV. SUMMARY

In summary, we have found a symmetry relationship in tunneling between two nuclei. For a parabolic potential, it is proved analytically that the summation of the one-dimensional tunneling probability at incident energies $V_B + \delta E$ and $V_B - \delta E$ is unity. It is also proved numerically that the symmetry relationship works rather well, although not exactly, for realistic nuclear potentials. The SymWKB formula is demonstrated to have more accurate predictions than the HW formula at the sub-barrier energy region and Kemble's WKB formula at the above-barrier energy region in different cases. It is also demonstrated that the multichannel tunneling probability at the above-barrier energy region can be predicted in the same way under the eigenchannel approximation, which produces undistinguished results compared to those of the Exact method. Moreover, the SymWKB method presented here for fusion reactions serves as an illustrative example. If we substitute the WKB method with the Exact method at below-barrier energies, it is evident that the SymExact method will also exhibit good performance at above-barrier energies based on the symmetry tunneling relationship. Because the WKB method is simpler than the Exact method, which involves solving the Schrödinger equation, it has great potential

to reduce computational time, particularly when dealing with more than hundreds of coupled channels such as in studying the influence of single-particle dissipation effects on fusion reactions [54]. The well extension of the symmetry tunneling law to the Eckart potential is also revealed. Due to the simple form and the accuracy of the symmetry relationship, the new SymWKB tunneling formula can be used to improve the realistic calculations in many fields [28–32]. Despite its effectiveness, the root cause behind this symmetrical tunneling phenomenon, and if there exist more general symmetry tunneling laws, still needs to be uncovered to understand the quantum mechanism.

ACKNOWLEDGMENTS

We thank Profs. A. K. Nasirov and N. Wang for important instructive comments that improved the manuscript. This work is supported by the National Key R&D Program of China (Contract No. 2022YFA1602302), the National Natural Science Foundation of China (Grants No. 12375130, No. 12235020, No. 12275360, No. 12175314, No. 12175313, and No. U2167204), the Continuous Basic Scientific Research Project, and the project supported by the Director's Foundation of Department of Nuclear Physics, China Institute of Atomic Energy (Grant No. 12SZJJ-202305).

-
- [1] R. Mohsen, *Quantum Theory Of Tunneling*, 2nd ed. (World Scientific, Singapore, 2013).
- [2] C. A. Bertulani, *Few-Body. Syst.* **56**, 727 (2015).
- [3] J. Ankerhold, *Quantum Tunneling in Complex Systems: The Semiclassical Approach* (Springer, Berlin, 2007).
- [4] N. Camus, E. Yakaboylu, L. Fechner, M. Klaiber, M. Laux, Y. Mi, K. Z. Hatsagortsyan, T. Pfeifer, C. H. Keitel, and R. Moshhammer, *Phys. Rev. Lett.* **119**, 023201 (2017).
- [5] L. Yang, C. J. Lin, H. M. Jia, D. X. Wang, N. R. Ma, L. J. Sun, F. Yang, X. X. Xu, Z. D. Wu, H. Q. Zhang, and Z. H. Liu, *Phys. Rev. Lett.* **119**, 042503 (2017).
- [6] B. B. Back, H. Esbensen, C. L. Jiang, and K. E. Rehm, *Rev. Mod. Phys.* **86**, 317 (2014).
- [7] C. J. Lin, J. C. Xu, H. Q. Zhang, Z. H. Liu, F. Yang, and L. X. Lu, *Phys. Rev. C* **63**, 064606 (2001).
- [8] C. J. Lin, *Phys. Rev. Lett.* **91**, 229201 (2003).
- [9] H. M. Jia, C. J. Lin, F. Yang, X. X. Xu, H. Q. Zhang, Z. H. Liu, Z. D. Wu, L. Yang, N. R. Ma, P. F. Bao, and L. J. Sun, *Phys. Rev. C* **89**, 064605 (2014).
- [10] H. M. Jia, C. J. Lin, F. Yang, X. X. Xu, H. Q. Zhang, Z. H. Liu, Z. D. Wu, L. Yang, N. R. Ma, P. F. Bao, and L. J. Sun, *Phys. Rev. C* **90**, 031601(R) (2014).
- [11] H. Q. Zhang, C. L. Zhang, C. J. Lin, Z. H. Liu, F. Yang, A. K. Nasirov, G. Mandaglio, M. Manganaro, and G. Giardina, *Phys. Rev. C* **81**, 034611 (2010).
- [12] L. Landau and E. Lifshitz, *Quantum Mechanics*, Course of Theoretical Physics Vol. 3 (Pergamon Press, Elmsford, NY, 1958).
- [13] Z. Ahmed, *Phys. Rev. A* **47**, 4761 (1993).
- [14] B. Wang, K. Wen, W. J. Zhao, E. G. Zhao, and S. G. Zhou, *At. Data Nucl. Data Tables* **114**, 281 (2017).
- [15] P. W. Wen, C. J. Lin, H. M. Jia, L. Yang, F. Yang, D. H. Huang, T. P. Luo, C. Chang, M. H. Zhang, and N. R. Ma, *Phys. Rev. C* **105**, 034606 (2022).
- [16] Y. Chen, H. Yao, M. Liu, J. Tian, P. Wen, and N. Wang, *At. Data Nucl. Data Tables* **154**, 101587 (2023).
- [17] L. F. Canto, P. R. S. Gomes, R. Donangelo, J. Lubian, and M. S. Hussein, *Phys. Rep.* **596**, 1 (2015).
- [18] Y. Eisen and Z. Vager, *Nucl. Phys. A* **187**, 219 (1972).
- [19] K. Hagino and N. Takigawa, *Prog. Theor. Phys.* **128**, 1061 (2012).
- [20] P. W. Wen, O. Chuluunbaatar, A. A. Gusev, R. G. Nazmitdinov, A. K. Nasirov, S. I. Vinitzky, C. J. Lin, and H. M. Jia, *Phys. Rev. C* **101**, 014618 (2020).
- [21] O. Chuluunbaatar, A. A. Gusev, S. I. Vinitzky, A. G. Abrashkevich, P. W. Wen, and C. J. Lin, *Comput. Phys. Commun.* **278**, 108397 (2022).
- [22] L. Yang, C. J. Lin, H. Yamaguchi, A. M. Moro, N. R. Ma, D. X. Wang, K. J. Cook, M. Mazzocco, P. W. Wen, S. Hayakawa, J. S. Wang, Y. Y. Yang, G. L. Zhang, Z. Huang, A. Inoue, H. M. Jia, D. Kahl, A. Kim, M. S. Kwag, M. L. Commará *et al.*, *Nat. Commun.* **13**, 7193 (2022).
- [23] S. Yusa, K. Hagino, and N. Rowley, *Phys. Rev. C* **85**, 054601 (2012).
- [24] K. Hagino and A. B. Balantekin, *Phys. Rev. A* **70**, 032106 (2004).
- [25] V. V. Sargsyan, S. Y. Grigoryev, G. G. Adamian, and N. V. Antonenko, *Comput. Phys. Commun.* **233**, 145 (2018).
- [26] A. J. Toubiana, L. F. Canto, and M. S. Hussein, *Eur. Phys. J. A* **53**, 34 (2017).
- [27] D. M. Brink and U. Smilansky, *Nucl. Phys. A* **405**, 301 (1983).
- [28] A. Nasirov, A. Fukushima, Y. Toyoshima, Y. Aritomo, A. Muminov, S. Kalandarov, and R. Utamuratov, *Nucl. Phys. A* **759**, 342 (2005).
- [29] S. Goriely, N. Chamel, and J. M. Pearson, *Phys. Rev. Lett.* **102**, 152503 (2009).
- [30] D. N. Poenaru, R. A. Gherghescu, and W. Greiner, *Phys. Rev. Lett.* **107**, 062503 (2011).
- [31] N. Schunck and L. M. Robledo, *Rep. Prog. Phys.* **79**, 116301 (2016).
- [32] S. A. Alavi, V. Dehghani, and M. Sayahi, *Nucl. Phys. A* **977**, 49 (2018).
- [33] E. C. Kemble, *Phys. Rev.* **48**, 549 (1935).
- [34] F. Cooper, A. Khare, and U. Sukhatme, *Phys. Rep.* **251**, 267 (1995).
- [35] D. L. Hill and J. A. Wheeler, *Phys. Rev.* **89**, 1102 (1953).
- [36] V. I. Zagrebaev, *Phys. Rev. C* **67**, 061601(R) (2003).
- [37] Y. E. Penionzhkevich, V. I. Zagrebaev, S. M. Lukyanov, and R. Kalpakchieva, *Phys. Rev. Lett.* **96**, 162701 (2006).
- [38] P. W. Wen, Z. Q. Feng, C. Li, C. J. Lin, and F. S. Zhang, *Chin. Phys. Lett.* **34**, 042501 (2017).
- [39] W. Brenig and R. Russ, *Surf. Sci.* **315**, 195 (1994).
- [40] C. H. Dasso, S. Landowne, and A. Winther, *Nucl. Phys. A* **407**, 221 (1983).
- [41] C. H. Dasso and S. Landowne, *Comput. Phys. Commun.* **46**, 187 (1987).
- [42] M. Dasgupta, A. Navin, Y. K. Agarwal, C. V. K. Baba, H. C. Jain, M. L. Jhingan, and A. Roy, *Nucl. Phys. A* **539**, 351 (1992).

- [43] G. Montagnoli, A. M. Stefanini, H. Esbensen, C. L. Jiang, L. Corradi, S. Courtin, E. Fioretto, J. Grebosz, F. Haas, H. M. Jia, M. Mazzocco, C. Michelagnoli, T. Mijatović, D. Montanari, C. Parascandolo, F. Scarlassara, E. Strano, S. Szilner, and D. Torresi, *Phys. Rev. C* **90**, 044608 (2014).
- [44] J. R. Leigh, M. Dasgupta, D. J. Hinde, J. C. Mein, C. R. Morton, R. C. Lemmon, J. P. Lestone, J. O. Newton, H. Timmers, J. X. Wei, and N. Rowley, *Phys. Rev. C* **52**, 3151 (1995).
- [45] A. Winther, *Nucl. Phys. A* **594**, 203 (1995).
- [46] P. W. Wen, C. J. Lin, R. G. Nazmitdinov, S. I. Vinitzky, O. Chuluunbaatar, A. A. Gusev, A. K. Nasirov, H. M. Jia, and A. Góźdz, *Phys. Rev. C* **103**, 054601 (2021).
- [47] K. Hagino, N. Rowley, and A. T. Kruppa, *Comput. Phys. Commun.* **123**, 143 (1999).
- [48] A. K. Nasirov, B. M. Kayumov, G. Mandaglio, G. Giardina, K. Kim, and Y. Kim, *Eur. Phys. J. A* **55**, 29 (2019).
- [49] A. A. Gusev, O. Chuluunbaatar, S. I. Vinitzky, and A. G. Abrashkevich, *Comput. Phys. Commun.* **185**, 3341 (2014).
- [50] S. I. Vinitzky, P. W. Wen, A. A. Gusev, O. Chuluunbaatar, R. G. Nazmitdinov, A. K. Nasirov, C. J. Lin, H. M. Jia, and A. Góźdz, *Acta Phys. Pol. B Proc. Suppl.* **13**, 549 (2020).
- [51] O. Chuluunbaatar, A. A. Gusev, A. G. Abrashkevich, A. Amaya-Tapia, M. S. Kaschiev, S. Y. Larsen, and S. I. Vinitzky, *Comput. Phys. Commun.* **177**, 649 (2007).
- [52] A. Diaz-Torres, *Phys. Rev. C* **81**, 041603(R) (2010).
- [53] L. Naderi and H. Hassanabadi, *Eur. Phys. J. Plus* **131**, 133 (2016).
- [54] E. Piasecki, M. Kowalczyk, S. Yusa, A. Trzcińska, and K. Hagino, *Phys. Rev. C* **100**, 014616 (2019).